Supporting Information

Yoshimura et al. 10.1073/pnas.0901184106

SI Text

Generation of *WSTF* Knockout Mice. *WSTF* genomic DNA fragments were obtained from the RP23–240H6 BAC clone by PCR. The targeting vector consisted of a 1.0-kb 5′ homologous region and a 10-kb 3′ homologous region, and the *neo* cassette was replaced with a 1.0-kb fragment containing an exon encoding the translation initiation site. Three targeted TT2 ES-cell clones (Wa-103–105), identified by Southern analysis using probes A and neo, were aggregated with single eight-cell embryos from CD-1 mice (1). Chimeric males were mated with C57BL/6 females and subsequent procedures were performed on a mixed C57BL/6×CBA background. Two lines exhibited the same phenotypic abnormalities. Offspring were genotyped either by Southern analysis using probe A, or by PCR using 3 specific primers that distinguished wild-type, heterozygous, and homozygous mice.

RT-PCR and Northern Blot Analysis. Total RNA from murine tissues and embryos was isolated with the ISOGEN kit (Wako) according to the manufacturer's protocol. For northern blot analyses (2), 30 μg of RNA was used with the indicated cDNA as a probe. For RT-PCR, cDNAs were generated by oligo dT-primed reverse transcriptase from 1 μg total RNA (3). PCR and real-time quantitative RT-PCR (qPCR) was performed as reported in ref. 4.

Flow Cytometric Analysis. The cell cycles of *WSTF*$^{-/-}$ and wild-type MEF cells were analyzed by flow cytometry as described in ref. 5. In brief, exponentially growing MEF cells were fixed with ethanol and DNA was stained with propidium iodide (PI). DNA content of each MEF cell was measured with a FACS Caliber analyzer (BD Bioscience).

Immunoprecipitation. After washing cells twice with ice-cold PBS, collected cells were resuspended in 1 mL of ice-cold lysis buffer [10 mM Tris·HCl (pH 7.4), 10 mM NaCl, 3 mM $MgCl_2$, and 0.5% (vol/vol) Nonidet P-40], incubated on ice for 30 min, and centrifuged for 5 min at 500 × *g*. Sedimented nuclear fractions were resuspended in TNE buffer [10 mM Tris·HCl (pH 7.5), 1% Nonidet P-40, 0.15 M NaCl, and 1 mM EDTA] and incubated for 30 min on ice. After centrifugation, the supernatants were used as whole cell extracts for immunoprecipitation by using anti-FLAG M2 affinity resin (Sigma) or the indicated antibodies with protein G Sepharose (GE Healthcare) followed by Western blot analysis with the indicated antibodies (3, 6, 7).

GST Pull-Down Assay. A series of transcription factors fused to GST were expressed in *E. coli*, as described in refs. 6 and 8. The predicted sizes of the expressed proteins were verified by SDS/PAGE. For the GST pull-down assays, bacterially expressed GST fusion proteins, or GST bound to glutathione-Sepharose 4B beads (GE Healthcare), were incubated for 2 h at 30 °C with [^{35}S]methionine-labeled proteins expressed by in vitro translation by using the TNT-coupled transcription-translation system (Promega). Free proteins were removed by washing the beads with NET-N^{+} buffer (150 mM NaCl, 1 mM EDTA, 20 mM Tris·HCl, pH 7.5, 0.5% Nonidet P-40, 1 mM PMSF, and 1 mM DTT). Bound proteins were eluted by boiling in SDS sample buffer and analyzed by 10% SDS/PAGE. After electrophoresis, radiolabeled proteins were visualized by using an image analyzer (BAS1500, Fuji).

1. Yoshizawa T, et al. (1997) Mice lacking the vitamin D receptor exhibit impaired bone formation, uterine hypoplasia and growth retardation after weaning. *Nat Genet* 16:391–396.
2. Takeyama K, et al. (1997) 25-Hydroxyvitamin D3 1alpha-hydroxylase and vitamin D synthesis. *Science* 277:1827–1830.
3. Kitagawa H, et al. (2003) The chromatin-remodeling complex WINAC targets a nuclear receptor to promoters and is impaired in Williams syndrome. *Cell* 113:905–917.
4. Nakamura T, et al. (2007) Estrogen prevents bone loss via estrogen receptor alpha and induction of Fas ligand in osteoclasts. *Cell* 130:811–823.
5. Takezawa S, et al. (2007) A cell cycle-dependent co-repressor mediates photoreceptor cell-specific nuclear receptor function. *EMBO J* 26:764–774.
6. Fujiki R, et al. (2005) Ligand-induced transrepression by VDR through association of WSTF with acetylated histones. *EMBO J* 24:3881–3894.
7. Ohtake F, et al. (2003) Modulation of oestrogen receptor signalling by association with the activated dioxin receptor. *Nature* 423:545–550.
8. Ohtake F, et al. (2007) Dioxin receptor is a ligand-dependent E3 ubiquitin ligase. *Nature* 446:562–566.
9. Sekine K, et al. (1999) Fgf10 is essential for limb and lung formation. *Nat Genet* 21:138–141.
10. Wang Z, et al. (2004) Polybromo protein BAF180 functions in mammalian cardiac chamber maturation. *Genes Dev* 18:3106–3116.

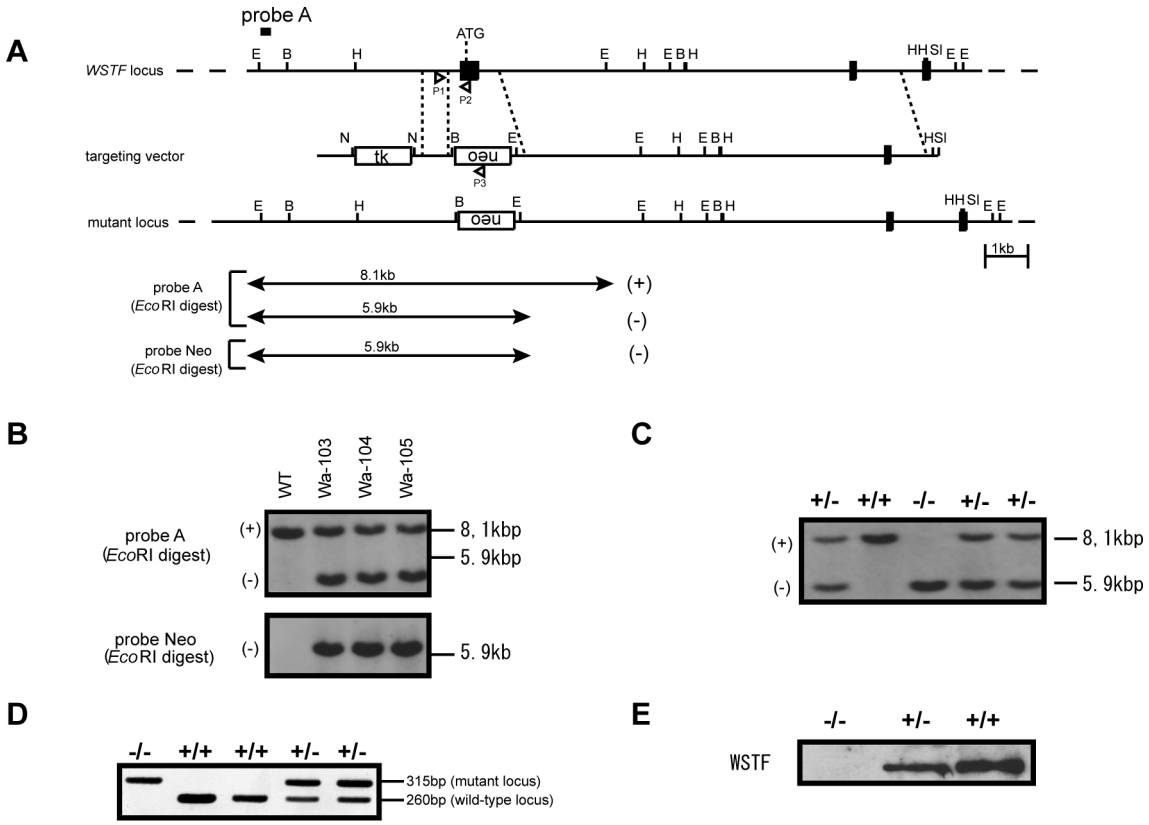

Fig. S1. Targeted disruption of the *WSTF* gene. (*A*) The targeted *WSTF* gene locus. Wild-type *WSTF* locus (*Top*), targeting vector (*Middle*), and predicted mutant locus (*Bottom*). Filled boxes indicate exons. Digested fragments detected by probe A and probe neo are indicated by arrows. B, *Bam*HI; E, *Eco*RI; H, *Hin*dIII; Sl, *Sal*I. Mice were generated following our standard method as described in refs. 1 and 9. (*B*) Southern blot analysis of targeted ES clones. Genomic DNA from wild-type TT2 cells (WT) and homologous targeted clones (Wa-103–105) were digested with *Eco*RI and hybridized to the external probe (probe A), or to the neo probe. (*C*) Southern blot analysis of tail DNA from the offspring of heterozygous litter mates with probe A as described for *B*. (*D*) PCR genotyping of E9.5 embryos using three primers (P1, P2, and P3) as indicated in *A*. Primer 1 and primer 2 were used to detect the wild-type allele (amplification of a 260-bp fragment). Primer 2 and primer 3 were used to detect the targeted allele (amplification of a 315-bp fragment). (*E*) Western blot analysis of WSTF protein from wild-type, heterozygote, and homozygote E10.5 embryos.

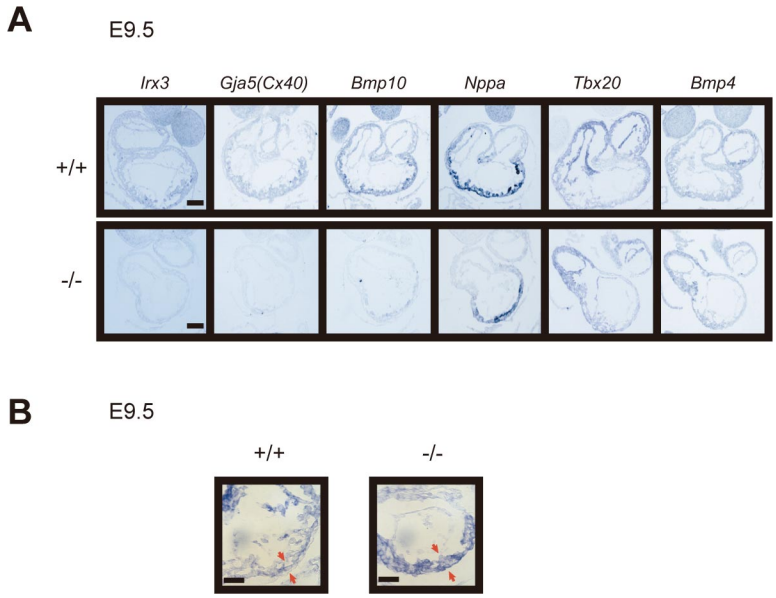

Fig. S2. Detailed analysis of cardiac phenotypes of *WSTF*$^{-/-}$ mice. (*A*) Decreased *Irx3*, *Gja5*, *Bmp10*, and *Nppa* expression in WSTF mutants at E9.5 as shown by section in situ hybridization. (*B*) Cardiac patterning defects with lack of trabeculations and multiple thicker myocardial layers (between arrowheads) are shown by *Tbx20* staining. [Scale bars, 100 μm in (*A*) and 10 μm in (*B*).]

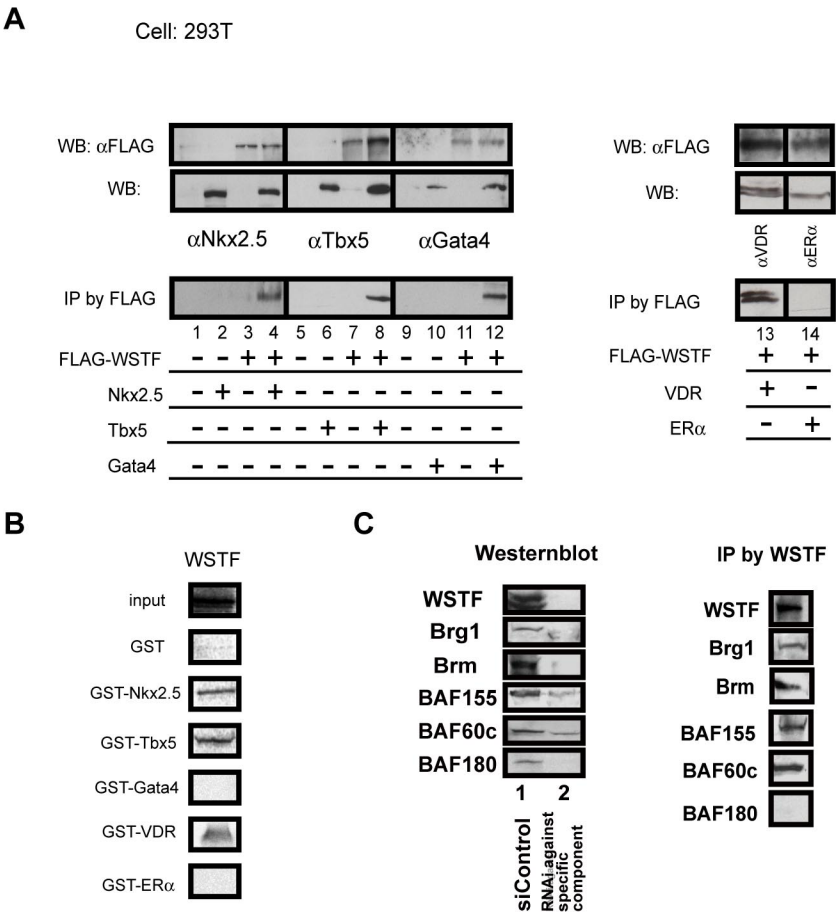

Fig. S3. In vitro analysis of the association between WSTF and cardiac transcription factors. (*A*) WSTF was coimmunoprecipitated with Nkx2.5, Tbx5, and Gata-4 in vivo. Coimmunoprecipitation was performed as described in refs. 3 and 6. (*B*) WSTF physically interacted with Nkx2.5 and Tbx5 but not with Gata4. A GST pull-down assay was performed as described in refs. 5 and 7. (*C*) The expression and the effect of siRNAs in P19.CL.6 cells (*Left*). Coimmunoprecipitation of WINAC components with WSTF in P19.CL.6 cells (*Right*).

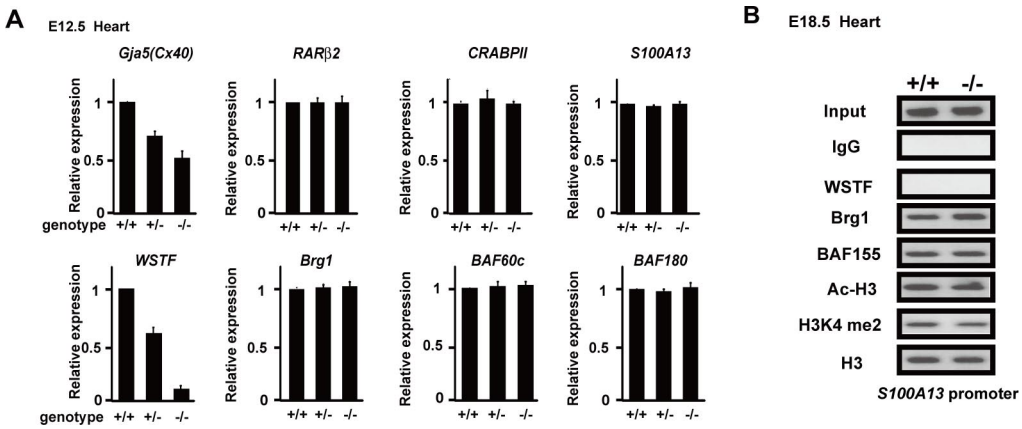

Fig. S4. Gene-specific regulation of WINAC compared with BAF180-containing PBAF complexes. (*A*) The expression of known target genes of a PBAF specific component (BAF180) (10) was not affected by *WSTF* ablation in E12.5 hearts. (*B*) PBAF components were recruited to the *S100A13* gene promoter regardless of the existence of WSTF. In vivo ChIP assays were performed with E18.5 hearts as shown in Fig. 3*E*.